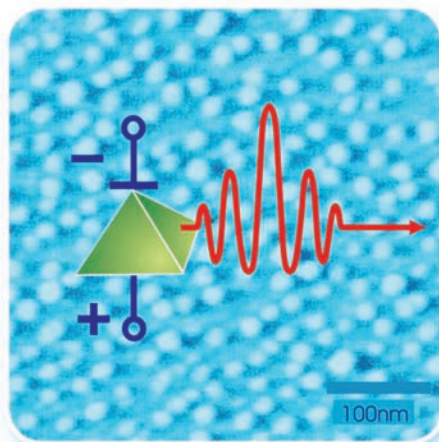
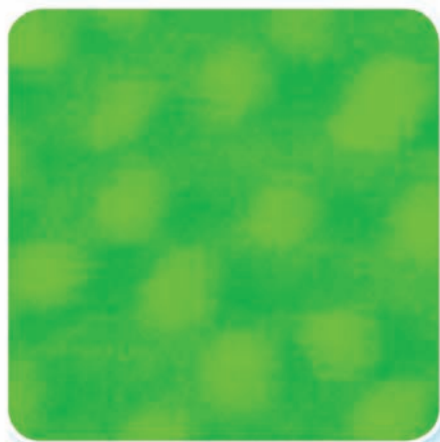
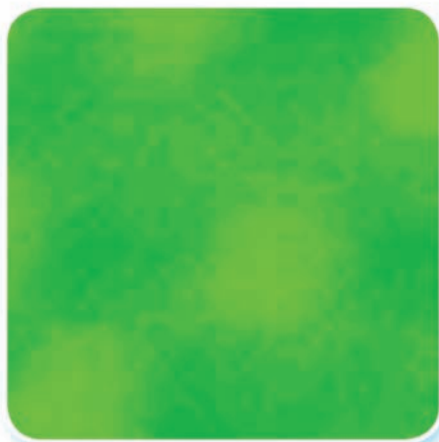
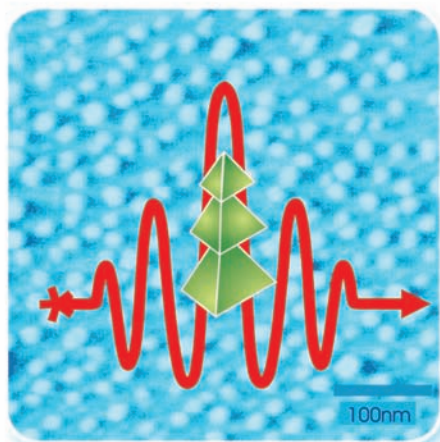


Edik U. Rafailov, Maria A. Cataluna,
Eugene A. Avrutin

 WILEY-VCH

Ultrafast Lasers Based on Quantum Dot Structures

Physics and Devices



*Edik U. Rafailov, Maria Ana
Cataluna, and Eugene A. Avrutin*

**Ultrafast Lasers Based on
Quantum Dot Structures**

Related Titles

Markel, V. A., George, T. F. (eds.)

Optics of Nanostructured Materials

568 pages

2008

E-Book

ISBN: 978-0-470-35349-3

Piprek, J. (ed.)

Nitride Semiconductor Devices: Principles and Simulation

519 pages with 220 figures and 53 tables

2007

Hardcover

ISBN: 978-3-527-40667-8

Champion, Y., Fecht, H.-J. (eds.)

Nano-Architected and Nanostructured Materials

Fabrication, Control and Properties

166 pages with 101 figures and 16 tables

2004

Online Book Wiley Interscience

ISBN: 978-3-527-60601-6

Harrison, P.

Quantum Wells, Wires and Dots

Theoretical and Computational Physics

480 pages

2000

Hardcover

ISBN: 978-0-471-98495-5

*Edik U. Rafailov, Maria Ana Cataluna,
and Eugene A. Avrutin*

Ultrafast Lasers Based on Quantum Dot Structures

Physics and Devices



**WILEY-
VCH**

WILEY-VCH Verlag GmbH & Co. KGaA

The Authors

Prof. Edik U. Rafailov

University of Dundee
Photonics and Nanoscience Gr.
Dundee, UK
e.u.rafailov@dundee.ac.uk

Dr. Maria Ana Cataluna

University of Dundee
Photonics and Nanoscience Gr.
Dundee, UK
M.A.Cataluna@dundee.ac.uk

Dr. Eugene A. Avrutin

University of York
Department of Electronics
York, UK
eaa2@ohm.york.ac.uk

All books published by Wiley-VCH are carefully produced. Nevertheless, authors, editors, and publisher do not warrant the information contained in these books, including this book, to be free of errors. Readers are advised to keep in mind that statements, data, illustrations, procedural details or other items may inadvertently be inaccurate.

Library of Congress Card No.: applied for

British Library Cataloguing-in-Publication Data

A catalogue record for this book is available from the British Library.

Bibliographic information published by the Deutsche Nationalbibliothek

The Deutsche Nationalbibliothek lists this publication in the Deutsche Nationalbibliografie; detailed bibliographic data are available on the Internet at <http://dnb.d-nb.de>.

© 2011 WILEY-VCH Verlag & Co. KGaA,
Boschstr. 12, 69469 Weinheim, Germany

All rights reserved (including those of translation into other languages). No part of this book may be reproduced in any form – by photoprinting, microfilm, or any other means – nor transmitted or translated into a machine language without written permission from the publishers. Registered names, trademarks, etc. used in this book, even when not specifically marked as such, are not to be considered unprotected by law.

Cover Design Adam Design, Weinheim

Typesetting Thomson Digital, Noida, India

Printing and Binding

Printed in the Federal Republic of Germany
Printed on acid-free paper

ISBN: 978-3-527-40928-0

Contents

Introduction IX

Acknowledgments XI

1	Semiconductor Quantum Dots for Ultrafast Optoelectronics	1
1.1	The Role of Dimensionality in Semiconductor Materials	1
1.2	Material Systems Used	4
1.2.1	III–V Epitaxially Grown Quantum Dots	4
1.2.2	QD-Doped Glasses	6
1.2.3	Quantum Dashes	6
1.3	Quantum Dots: Distinctive Properties for Ultrafast Devices	7
1.3.1	Inhomogeneous Broadening	7
1.3.2	Ultrafast Carrier Dynamics	9
2	Foundations of Quantum Dot Theory	11
2.1	Energy Structure and Matrix Elements	11
2.2	Theoretical Approaches to Calculating Absorption and Gain in Quantum Dots	14
2.3	Kinetic Theory of Quantum Dots	22
2.4	Light–Matter Interactions in Quantum Dots	37
2.5	The Nonlinearity Coefficient	51
3	Quantum Dots in Amplifiers of Ultrashort Pulses	55
3.1	Optical Amplifiers for High-Speed Applications: Requirements and Problems	55
3.2	Quantum Dot Optical Amplifiers: Short-Pulse Operating Regime	62
3.3	Quantum Dot Optical Amplifiers at High Bit Rates: Low Distortions and Patterning-Free Operation	63
3.4	Nonlinear Operation and Limiting Function Using QD Optical Amplifiers	76

4	Quantum Dot Saturable Absorbers	77
4.1	Foundations of Saturable Absorber Operation	77
4.2	The General Physical Principles of Saturable Absorption in Semiconductors	80
4.2.1	Physical Processes in a Saturable Absorber	80
4.2.2	Geometry of Saturable Absorber: SESAM versus Waveguide Absorber – The Cavity Enhancement of Saturable Absorption and the Standing Wave Factor in SESAMs	84
4.3	The Main Special Features of a Quantum Dot Saturable Absorber Operation	87
4.3.1	Bandwidth of QD SAs	88
4.3.2	Dynamics of Carrier Relaxation: Ultrafast Recovery of Absorption	88
4.3.3	Saturation Fluence	94
5	Monolithic Quantum Dot Mode-Locked Lasers	99
5.1	Introduction to Semiconductor Mode-Locked Lasers	99
5.1.1	Place of Semiconductor Mode-Locked Lasers Among Other Ultrashort Pulse Sources	99
5.1.2	Mode-Locking Techniques in Laser Diodes: The Main Principles	100
5.1.3	Passive Mode Locking: The Qualitative Picture, Physics, and Devices	101
5.2	Theoretical Models of Mode Locking in Semiconductor Lasers	103
5.2.1	Small-Signal Time Domain Models: Self-Consistent Pulse Profile	103
5.2.2	Large-Signal Time Domain Approach: Delay Differential Equations Model	109
5.2.3	Traveling Wave Models	120
5.2.4	Frequency and Time–Frequency Treatment of Mode Locking: Dynamic Modal Analysis	125
5.3	Main Predictions of Generic Mode-Locked Laser Models and their Implication for Quantum Dot Lasers	126
5.3.1	Laser Performance Depending on the Operating Point	126
5.3.2	Main Parameters that Affect Mode-Locked Laser Behavior	129
5.4	Specific Features of Quantum Dot Mode-Locked Lasers in Theory and Modeling	131
5.4.1	Delay Differential Equation Model for Quantum Dot Mode-Locked Lasers	132
5.4.2	Traveling Wave Modeling of Quantum Dot Mode-Locked Lasers: Effects of Multiple Levels and Inhomogeneous Broadening	141
5.4.3	Modal Analysis for QD Mode-Locked Lasers	153
5.5	Advantages of Quantum Dot Materials in Mode-Locked Laser Diodes	154
5.5.1	Advantages of QD Saturable Absorbers	154
5.5.2	Broad Gain Bandwidth	154
5.5.3	Low Threshold Current	155
5.5.4	Low Temperature Sensitivity	155

5.5.5	Suppressed Carrier Diffusion	156
5.5.6	Lower Level of Amplified Spontaneous Emission	157
5.5.7	Linewidth Enhancement Factor	157
5.6	Ultrashort Pulse Generation: Achievements and Strategies	158
5.6.1	Monolithic Mode-Locked Quantum Dot Lasers	158
5.6.2	Chirp Measurement and Pulse Compression	161
5.6.3	Toward Higher Power: Tapered Lasers	164
5.6.4	Toward Higher Repetition Rates	165
5.6.5	External Cavity QD Mode-Locked Lasers	166
5.7	Noise Characteristics of QD Mode-Locked Lasers	167
5.7.1	Timing Jitter	167
5.7.2	Pulse Repetition Rate Stability and Resilience to Optical Feedback	170
5.7.3	Performance Under Optical Injection	172
5.8	Performance of QD Mode-Locked Lasers at Elevated Temperature	174
5.8.1	Stable Mode Locking at Elevated Temperature	174
5.8.2	Pulse Duration Trends at Higher Temperatures	175
5.8.3	The Use of p-Doping in QD Mode-Locked Lasers	176
5.9	Exploiting Different Transitions for Pulse Generation	176
5.9.1	Mode Locking via Ground and Excited States	176
5.9.2	The Excited-State Transition as Tool for Novel Mode-Locking Regimes	179
5.10	Summary and Outlook	180
5.10.1	QD Mode-Locked Laser Diodes: New Functionalities	180
5.10.2	Future Directions	181
6	Ultrashort Pulse Solid State Lasers Based on Quantum Dot Saturable Absorbers	183
6.1	A Brief Historical Overview of Ultrashort-Pulse Generation	183
6.2	Macroscopic Parameters of Saturable Absorbers	184
6.3	QD SESAMs for Efficient Passive Mode Locking of Solid-State Lasers Emitted around 1 μm	187
6.4	QD SESAMs for Efficient Passive Mode Locking of Solid-State Lasers Emitted around 1.3 μm	193
6.5	QD SESAMs for the Passive Mode Locking of Fiber Lasers	199
6.6	Mode-Locked Semiconductor Disk Lasers Incorporating QD SESAMs	201
6.7	Optically Pumped Quantum Dot VECSELS	204
7	Saturable Absorbers Based on QD-Doped Glasses	207
7.1	II–VI Semiconductor Nanocrystals in Glass	207
7.2	IV–VI Semiconductor QD-Doped Glasses for Ultrashort-Pulse Generation from Solid-State Lasers	209
7.3	QD-Doped Glass Saturable Absorbers for Passive Mode Locking around 1.3 μm	210

7.4	Cr:YAG Laser Passively Mode Locked with a QD-Doped Glass Saturable Absorber	212
7.5	PbS QD-Doped Glass Saturable Absorbers for Passive Mode Locking around 1 μm and Their Nonlinear Characteristics	214
8	Emerging Applications of Ultrafast Quantum Dot Lasers	217
8.1	Optical Communications	217
8.2	Datacoms	219
8.3	Biophotonics and Medical Applications	220
8.4	Outlook	220
	References	223
	Index	241

Introduction

Over the past three decades, laser physics has advanced dramatically owing to the efforts of scientists and technologists. Refined laser operation in continuous wave (cw) or quasi-cw (i.e., pumped by current pulses longer than the characteristic times of the laser dynamics) regimes has been accompanied by reliable techniques for the generation of periodic sequences of ultrashort optical pulses.

Mode locking is a technique that facilitates the generation of the shortest pulse durations and the highest repetition rates available from ultrafast lasers. The basis of this methodology lies in locking the phases of the longitudinal modes of a laser resonator. Summing all the mode frequencies with a fixed phase relationship results in a periodic sequence of intense ultrashort pulses with a repetition rate related inversely to the cavity round-trip time. The locking of the phases can be achieved either through an applied modulation of the losses or gain in the laser or by exploitation of nonlinearities such as the optical Kerr effect in some crystal-based laser systems. Mode locking is a well-established technique and routine generation of ultrashort pulses is now available from a wide range of lasers, with Kerr-lens mode-locked solid-state lasers (notably titanium-doped sapphire) producing the shortest pulses to date in the near-infrared spectral region.

Access to practical femtosecond lasers and related sources has opened up a range of applications from real-time monitoring of chemical reactions [1] to ultrahigh bit rate optical communications [2, 3], thereby enabling the realization of new concepts in ultrafast optical networking, signal processing, and information transmission [4]. Compact, mass-produced lasers having multigigahertz repetition rates are becoming key components in photonic switching devices, optical interconnects, and clock distribution in integrated circuits [5]; ultrafast electro-optical sampling [6]; and high-speed analogue-to-digital converters [7, 8]. The enormous impact of ultrafast optical sources has already been recognized in the form of two Nobel Prizes awarded to A. Zewail (1999) and T. Hansch (2005) for applications in femtochemistry and laser-based precision spectroscopy, respectively [9, 10].

To increase the applicability of ultrafast optical sources, a number of research groups have been exploring the alternatives to Ti:sapphire and similar lasers, which

tend to be rather bulky and inefficient. Semiconductor lasers represent one of the most exciting options for the generation of femtosecond optical pulses because these offer admirable potential for compactness and integrability as well as excellent prospects for direct electrical control. The mode locking of semiconductor diode lasers (at present, mainly based on quantum well heterostructures) by active and passive modulation of cavity losses is an established technique for the generation of picosecond and high repetition rate optical pulses in the near-infrared spectral range [11, 12]. In many cases, it is possible to incorporate the components required for passive mode locking directly into the device structure, thereby further simplifying the fabrication techniques. Progress in semiconductor laser development has led to the production of ultrashort and high repetition rate pulses from simple system configurations that, although not easily achieving the femtosecond pulse durations that are routinely available from the diode-pumped crystal-based lasers, are showing promise for efficient and controllable operation in ultrafast regimes from electrically pumped devices. Novel structures based on quantum dots have enhanced the characteristics of these lasers further and opened up new possibilities in ultrafast science and technology by enabling the generation and amplification of femtosecond optical pulses directly from laser diode devices, thus providing a cost-efficient pulse source [13].

Furthermore, quantum dot-based materials that demonstrate ultrabroadband absorption and ultrafast carrier dynamics are currently one of the most promising materials for the design of ultrafast saturable absorbers that have been employed in a wide range of laser systems, turning them into more compact, reliable, and inexpensive optical sources.

In this book, we summarize the progress and recent results in the development of efficient and compact ultrafast laser and amplifier devices based on quantum dot materials and structures. To better understand the potential of quantum dot devices, we start with a brief introduction to these materials and highlight the unique characteristics that make these low dimensional materials attractive for ultrafast applications (Chapter 1). In Chapter 2, we lay the foundations of quantum dot theory that are necessary for the following chapters. Chapters 3 and 4 will focus on the physics and state of the art in quantum dot-based optical amplifiers and saturable absorbers that are compatible with ultrashort pulses, respectively. Chapter 5 accounts for the main achievements in the generation of ultrashort pulses directly from quantum dot semiconductor diode lasers. In Chapter 6, an overview of some applications of quantum dot-based saturable absorbers in a number of mode-locked lasers is provided. Besides, a short overview of the recent progress in quantum dot vertical external cavity surface emitting lasers is also given. Chapter 7 will report on the progress of quantum dot in glass saturable absorbers. Finally, in Chapter 8, we conclude with an analysis of emerging future applications of ultrafast quantum dot lasers. The reader is expected to have reasonable knowledge of semiconductor physics and laser principles, with the particulars related to both the ultrafast pulse generation and propagation and the quantum dots presented in the relevant chapters.

Acknowledgments

Particular thanks go to E.V. Viktorov at Université Libre de Bruxelles for carefully reading most parts of the manuscript and making invaluable suggestions, not to mention extremely useful discussions. We are also grateful to I. Montrosset at Politecnico di Torino, A. Vladimirov at WIAS Berlin, and H. Simos at the University of Athens for useful discussions of some of the theoretical aspects of the book and to W. Sibbett and A. Lagatsky at St Andrews University for stimulating discussions on the experimental aspects. We are very grateful to V. Ustinov at Ioffe Institute (St Petersburg) and D. Livshits at Innolume GmbH (Dortmund) for providing us the samples used in our experimental studies and for fruitful discussion of experimental methodologies. Finally, we are grateful to all the authors (and publishers) who gave their consent to reproduce the figures representing their results in this book, and, last but not least, to all the staff at John Wiley & Sons, Inc. (particularly V. Molière and A. Tschörtner) for their helpfulness and patience.

The authors acknowledge the financial support from European Community's Seventh Framework Programme FAST-DOT under grant agreement 224338 and the UK Engineering and Physical Sciences Research Council (EPSRC).

M.A. Cataluna also acknowledges the financial support from the Royal Academy of Engineering/EPSCR Research Fellowship.

1

Semiconductor Quantum Dots for Ultrafast Optoelectronics

1.1

The Role of Dimensionality in Semiconductor Materials

The history of semiconductor lasers has been punctuated by dramatic revolutions. Several proposals of injection semiconductor lasers were studied between the late 1950s and the early 1960s, and the first demonstrations of p–n junction GaAs lasers followed in 1962 [14]. Until the 1980s, only bulk materials were used in semiconductor devices. Originally, these were homostructure devices, functionalized by a doping profile including a p–n junction in the same material. However, these lasers exhibited very low efficiency due to high optical and electrical losses. At that time, pioneers such as Alferov and Kroemer independently proposed a laser construction known as the double heterostructure and involving an active layer of a semiconductor with a relatively narrow bandgap layer surrounded by two injector layers of more broadband material [15]. Such a design offers several crucial advantages. First, it efficiently localizes the charge carriers of both signs (electrons and holes) within the active layer, by creating a potential well for both types of carriers. This potential well also leads to the possibility of achieving carrier densities in the active layer exceeding the doping level of the injector layers (the superinjection effect); thus, low-doped injectors can be used and the optical losses are significantly decreased compared to those in early homostructure lasers, which were by necessity highly doped. Second, as narrowband materials tend to have a higher refractive index, the electronic confinement is accompanied by the *optical* confinement, with an epitaxially determined waveguide formed in the transverse direction (perpendicular to the plane of the epitaxial layers). In the simplest version of a double heterostructure, the active layer doubles as the waveguide core; most structures currently used, including quantum dot (QD) lasers, use a *separate confinement* arrangement whereby the relatively thin active layer is embedded in the broader *optical confinement layer* (made of a broader bandgap material to localize the carriers in the active layer), which, in its turn, is sandwiched between two cladding (p- and n-emitter) layers. These have a still broader bandgap and thus, importantly, a lower refractive index than that of the optical confinement layer to provide the optical confinement/waveguiding.

The enhanced electronic and optical confinement (localization) in the double heterostructure drastically improved the operational characteristics of laser diodes, in particular the threshold current density (current per unit area) J_{th} , which decreased by as much as two orders of magnitude.

Another revolution followed when it was realized that the confinement of electrons to lower dimensional semiconductor structures translates into completely new optoelectronic properties, compared to bulk semiconductors. The obvious can therefore be asked: how small should this confinement be? To answer this question, one should recall the concept of the de Broglie wavelength of thermalized electrons λ_B , as shown in Equation 1.1:

$$\lambda_B = \frac{h}{p} = \frac{h}{\sqrt{2m^*E}}, \quad (1.1)$$

where h is Planck's constant, p is the electron momentum, m^* is the electron effective mass, and E is the energy.

In the case of III–V compound semiconductors (such as the AlGaAs and InGaAsP material systems), λ_B is typically on the order of tens of nanometers for carriers with typical thermal energies [16]. Therefore, if one of the dimensions of a semiconductor is comparable to, or less than λ_B , the electrons will be confined to two dimensions and so the energy–momentum relations will dramatically change because quantization effects start to take place in one of the dimensions. This is the case for charge carriers in a quantum well (QW) structure, which have been intensively studied since the 1970s and are now prevalent in semiconductor lasers and, to a lesser degree, in amplifiers.

The next stage in reducing dimensionality in a semiconductor active medium is the quantum wire (QWR), which is a one-dimensional confined structure in the sense that the carrier movement is free in one dimension and confined in two others. Quantum wires can be fabricated by direct lithographic methods, but possibly the most important one-dimensionally confined structure from the laser device perspective is the quantum dash (QDH) structure considered in more detail below.

Finally, a quantum dot is a nanostructure in which the electron and hole movement is confined in all the three dimensions. Quantum dots are thus tiny clusters of semiconductor material having all three dimensions of only a few nanometers.

The spatial confinement of the carriers in lower dimensional semiconductors leads to dramatically different energy–momentum relations in the directions of confinement, which results in completely new density of states, compared to the bulk case, as depicted in Figure 1.1.

As dimensionality decreases, the density of states is no longer continuous or quasi-continuous but becomes quantized. In the case of quantum dots, the charge carriers occupy only a restricted set of energy levels rather like the electrons in an atom, and for this reason, quantum dots are sometimes referred to as “artificial atoms.” It is important to stress, however, that QDs actually contain hundreds of thousands of atoms.

For a given energy range, the number of carriers necessary to fill out these states reduces substantially as the dimensionality decreases, which implies that it becomes

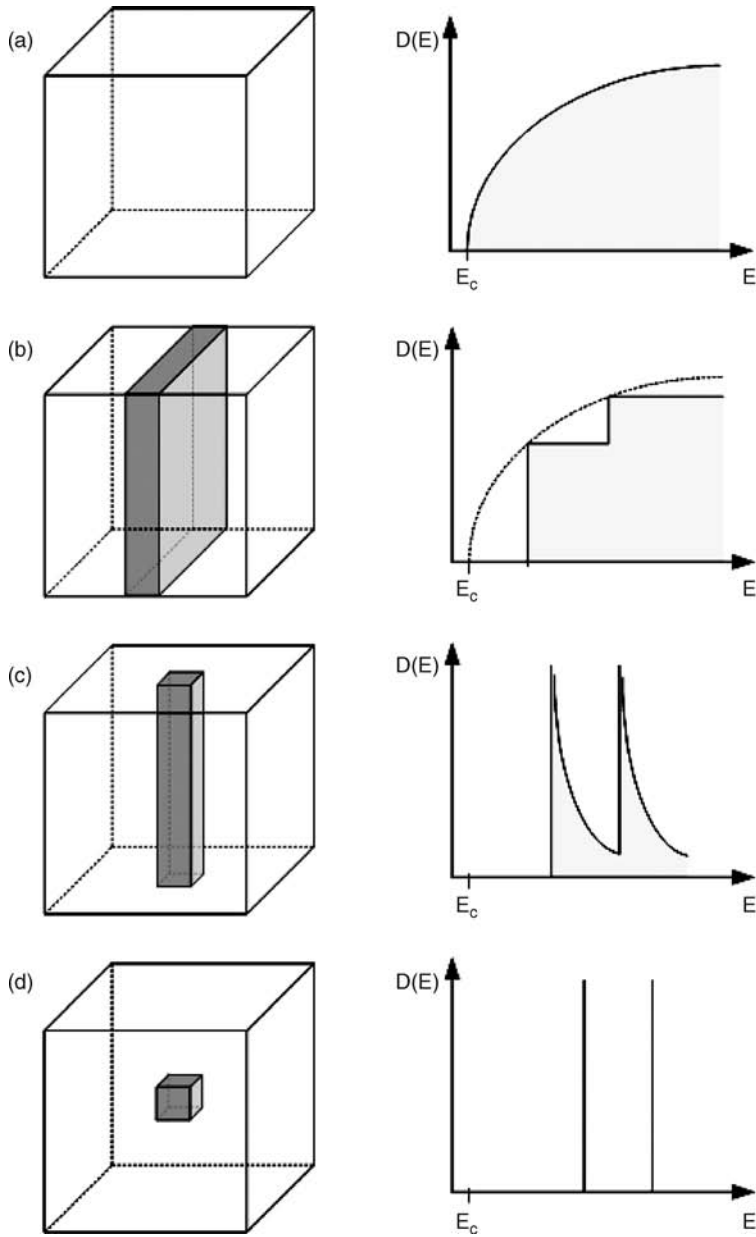


Figure 1.1 (Right) Schematic morphology and (left) density of states for charge carriers in semiconductor structures with different dimensionalities: (a) bulk, (b) quantum well, (c) quantum wire, and (d) quantum dot.

easier to achieve transparency and, eventually, the inversion of population needed to achieve optical gain and thus laser operation – with the resulting reduction of the threshold current density J_{th} of a laser. In fact, the reduction in J_{th} has been quite spectacular over the years, with sudden jumps whenever the dimensionality is decreased [15]. Low-dimensional lasers also exhibit reduced temperature sensitivity of J_{th} , and in the case of quantum dots, an infinite characteristic temperature has even been predicted.

The implications of a quantized density of states for QDs are immense and were identified as early as 1976 when a QD laser was first proposed [17]. A subsequent theoretical treatment was published in 1982 [18] in which it was predicted that the ideal three-dimensional localization of carriers would translate into a low-threshold, temperature-insensitive, and single-frequency laser. The latter two predictions relied, however, on the assumption of the dots being nearly identical and this having almost the same energy level separation (weak inhomogeneous broadening). While realization of such QD systems may yet become possible in future, all the dot structures grown so far have a significant size (and possibly composition) dispersion, leading to a significant inhomogeneous broadening of the emission line. Thus, some of the initial expectations from QD laser, such as the single-frequency lasing, had to be revised, while others, such as application for ultrafast optoelectronics, became more feasible. This will be discussed in more detail in Chapter 2, which will present a summary of quantum dot theory concentrating on the areas of interest to the subject of short pulse generation and amplification.

1.2

Material Systems Used

A variety of materials have been used in the past in the fabrication of quantum dots. In the following sections, we will describe the main QD material systems that have shown particular promise for ultrafast optoelectronic applications.

1.2.1

III–V Epitaxially Grown Quantum Dots

Since the pioneering work reported in 1985 [19], where the formation of InAs clusters in a GaAs matrix was demonstrated, a number of groups have synthesized and studied self-organized QD structures in a range of distinctive systems [20]. One of such groups of materials is based on III–V QDs, epitaxially grown on a semiconductor substrate. To date, the most promising results have been achieved through the spontaneous formation of three-dimensional islands during strained layer epitaxial growth – a process known as the Stranski–Krastanov mechanism. In this process, when a film is epitaxially grown over a substrate, the initial growth occurs layer by layer, but beyond a certain critical thickness, three-dimensional islands begin to form – the quantum dots. A continuous film, of quantum well thickness and usually assumed to have quantum well properties, lies underneath the dots and is called the

wetting layer. A crucial requirement of this technique is that the lattice constant of the deposited material is larger than that of the substrate, so that the additional strain leads to the formation of clusters. This is the case of an InAs film (lattice constant of 6.06 Å) on a GaAs substrate (lattice constant of 5.64 Å) or on an InP substrate (lattice constant of 5.87 Å). Many different systems can be grown using this technique and these are not limited to group III–V constituents.

Despite being an extremely complex process, the Stranski–Krastanov mode is now widely used in the self-assembly of quantum dots. Epitaxial quantum dot materials can be grown using molecular beam epitaxy (MBE) and metal organic chemical vapor deposition (MOCVD). These techniques have been extensively used in the past decades to grow QW materials and therefore the growth of QDs benefited immensely from well-established procedures. This aspect is also advantageous for commercialization, as manufacturers do not need to invest in new epitaxy equipment to fabricate these structures.

Stranski–Krastanov-grown quantum dots typically have a pyramidal shape, with a base of 15–20 nm and a height of the order of ~ 5 nm (it is possible that after overgrowth, this shape is modified). At present, the densities of quantum dots lie typically between 10^9 and 10^{12} cm $^{-2}$. The relatively sparse distribution of quantum dots results in a low value of gain. Thus, the levels of gain and optical confinement provided by a single layer of quantum dots may not be enough for the optimal performance of a laser. To circumvent this problem, quantum dot structures are routinely grown in stacks that allows an increase in the modal gain without increasing the internal optical mode loss [21]. Further optical confinement is enabled through the embedding of QD arrays within layers of higher refractive index and bandgap energy, therefore forming a heterostructure.

Figure 1.2a and b [22] shows a surface view of a system of self-organized QDs and a side view of a stack of three QD layers, respectively, to give an idea of dimensions, distances, and shapes of typical self-organized QDs in a practical device structure. In this case, the dot density in each layer is around 4×10^{10} cm $^{-2}$, with the lateral size of QDs of 15–18 nm. The apparent dot bases are almost square shaped and oriented along the $\langle 100 \rangle$ direction in the crystal, with a slight elongation along one of the $\langle 110 \rangle$

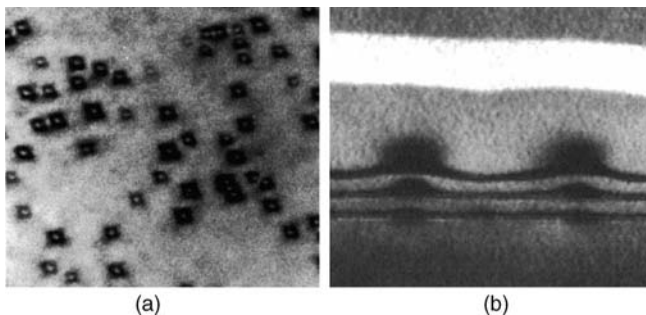


Figure 1.2 Scanning electron microscope image of a plan view (a) and side view (b) of a system of three-stacked QDs in a laser structure. Courtesy of D. Livshits, Innolume GmbH.

directions. Note also that the average size of the dots appears to increase from layer to layer, contributing to the inhomogeneous broadening as discussed below.

Materials based on InGaAs/InAs dots grown on a GaAs substrate have been investigated quite comprehensively in the past few years because their emission wavelengths can not only be tuned between 1.0 and 1.3 μm but can also be extended to 1.55 μm [20], through careful adjustment of the growth conditions. InGaAs/InAs QDs grown on InP substrate emit in the 1.4–1.9 μm wavelength range, thus enabling easy access to the optical communications band around 1.55 μm .

Epitaxially grown QD materials have been successfully deployed in the form of lasers, amplifiers, and saturable absorbers – and as such, they hold great promise for a complete optoelectronic integration of an array of distinct devices on the same wafer.

1.2.2

QD-Doped Glasses

QD-doped glasses represent the second key group of quantum dot materials that are of significant interest in ultrafast physics. These materials consist of semiconductor nanoparticles (such as PbS, PbSe, and CdTe) incorporated into a variety of transparent dielectric matrices, with excitonic absorption peaks in the spectral range of about 0.5–2.5 μm [23–25]. One of the main advantages of QD-doped glasses is that they are much cheaper and easier to produce than their epitaxially grown counterparts. QD-doped glasses have not yet realized their full potential as gain media in that efficient laser emission has not been observed to date. Moreover, they are not yet practical within the context of fabricated electrically injected devices. This material system is thus being investigated mainly as an absorber medium. QD-doped glasses have, in fact, been successfully used as ultrafast saturable absorbers and optical switches because they exhibit similar ultrafast properties to III–V QDs in heterostructures.

1.2.3

Quantum Dashes

Quantum dashes are often mentioned alongside quantum dots and are produced in a similar technological process, typically by growing InAs (notionally a few monolayers) on top of thin AlGaInAs/InP layers – such QDHs emit in the 1.55 μm wavelength band. However, the energy structure of quantum dashes is very different from those of quantum dots. Like QDs, QDHs have a vertical dimension of the order of 3–4 nm and a lateral dimension of 10–20 nm. However, unlike a QD, a QDH is elongated in the other lateral dimension, its typical length being on the order of fractions of a micron, which is considerably larger than the electron and hole de Broglie wavelengths. Therefore, two of the three components of the carrier wave vector in a QDH are quantized, but the third one is quasi-continuous, meaning that instead of discrete energy levels, like QDs, a single QDH has quasi-continuous energy bands for both electrons and holes, like bulk and QW materials, although the

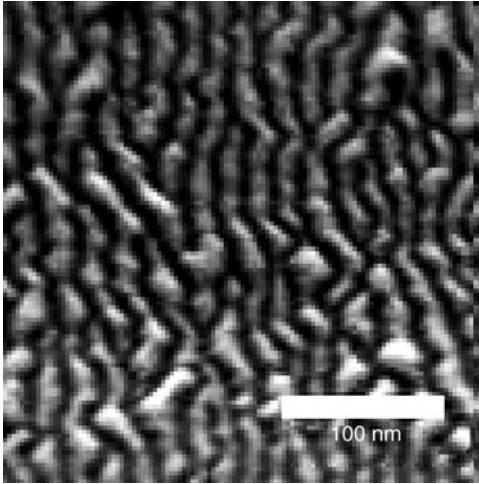


Figure 1.3 Scanning electron microscope image of a plan view of a sample of nonovergrown InAs quantum dashes. Reproduced with permission from Ref. [26].

density of states for electrons and holes has sharp peaks, reminiscent of the delta functions of QDs. In theoretical models, the properties of QDHs are quite well described [26] as similar to those of quantum wire assemblies with fluctuating transverse/lateral dimensions. This approach is not absolutely accurate because, unlike quantum wires, QDHs are self-assembled with a high density (hence there is a possibility of tunneling between them), and their geometry is more irregular than that of ideal quantum wires (an example is shown in Figure 1.3), but it has been shown in several papers that this irregularity does not significantly affect the QDH properties [26].

1.3

Quantum Dots: Distinctive Properties for Ultrafast Devices

1.3.1

Inhomogeneous Broadening

The main motivation behind the idea of a QD laser was to conceive a design for a low-threshold, single-frequency, and temperature-insensitive laser given the quantum nature of the density of states. Interestingly, practical devices exhibit the predicted outstandingly low thresholds [27, 28], but the spectral bandwidths of such lasers are significantly broader than those of conventional quantum well lasers [29]. This characteristic is attributable to *inhomogeneous broadening* with its dependence on the dot size distributions. Indeed, because of their self-organized growth, QDs exhibit a Gaussian distribution of sizes, with a corresponding, nearly Gaussian in the first approximation, distribution of emission frequencies. Also, fluctuations in the

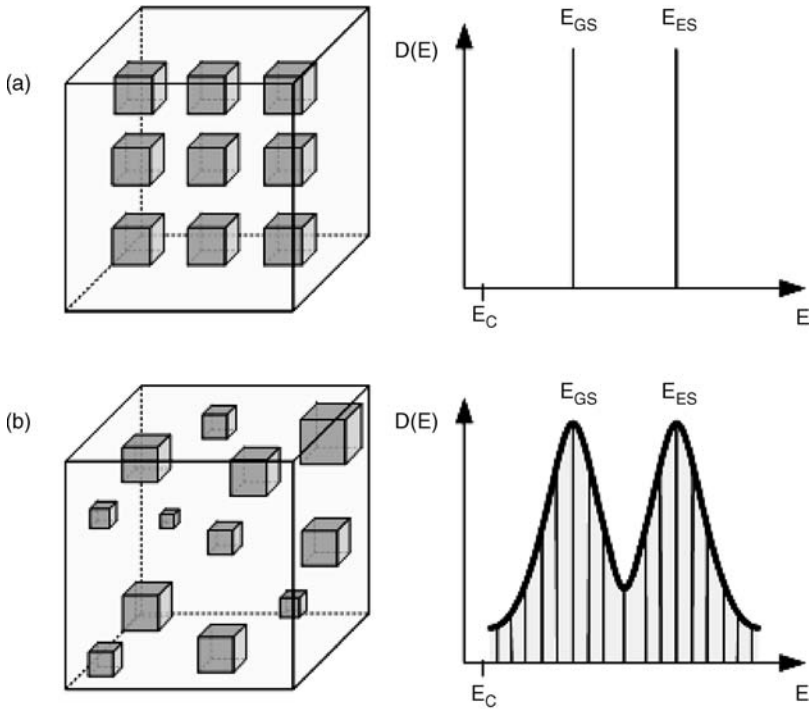


Figure 1.4 (Right) Schematic morphology and (left) density of states for charge carriers in (a) an ideal quantum dot system and (b) a real quantum dot system, where inhomogeneous broadening is illustrated.

elastic strain in different parts of the wafer will affect the level of energy [30]. The effects of inhomogeneous broadening on the density of states are schematically illustrated in Figure 1.4. The recent results from a number of research groups, including our own, indicate that because of this specific characteristic these structures could be designed to offer some advantages in ultrafast science and technology. This is because a very wide bandwidth is available for the generation, propagation, and amplification of ultrashort pulses, which can be tuned across a broad spectral latitude. Moreover, well-established growth technologies for such structures allow this broadening to be controlled and tailored by selecting QD layers with suitable size distributions [31, 32]. However, to date, only a small fraction of these possibilities have been realized, and optical pulses generated by quantum dot sources are one to two orders of magnitude longer than the inverse width of the inhomogeneously broadened gain spectrum. It is also important to stress that a highly inhomogeneously broadened gain also encompasses a number of disadvantages because it partially defeats the purpose of a reduced dimensionality, by broadening the density of states. Indeed, the fluctuation in the size of the QDs increases the transparency current and reduces the modal and differential gain [33, 34].

As for epitaxially grown QD layers, it has been shown that the variation in the dot size in QD-doped glasses leads to a change in the spectral location of the first excitonic absorption peak, giving a possibility of continuous absorption tuning to a substantial spectral extent [35].

1.3.2

Ultrafast Carrier Dynamics

In the initial studies of QD-based materials, it was thought that their charge carrier dynamics would be significantly slower than those of quantum well materials due to a phonon bottleneck effect [36, 37]. This effect was predicted on the basis that due to the discrete energy levels, electrons would not be able to relax via phonon interaction because it would not be possible to match the phonon energy; this expected limitation became known as *the phonon bottleneck*. Interestingly, experiments have demonstrated quite the opposite. As a consequence of access to a number of recombination paths for the carriers, QD structures exhibit ultrafast recovery times, under both absorption and gain conditions [38].

In several such assessments, the absorber dynamics of surface and waveguided QD structures were investigated by using a pump-probe technique (see, for example, Refs [39, 40]). This evaluation showed the existence of at least two distinct time constants for the recovery of the absorption. A fast recovery of around 1 ps is followed by a slower recovery process that extends to 100 ps (Figure 1.5). The fast recovery time is particularly useful for enabling saturable absorbers to mode lock lasers at high

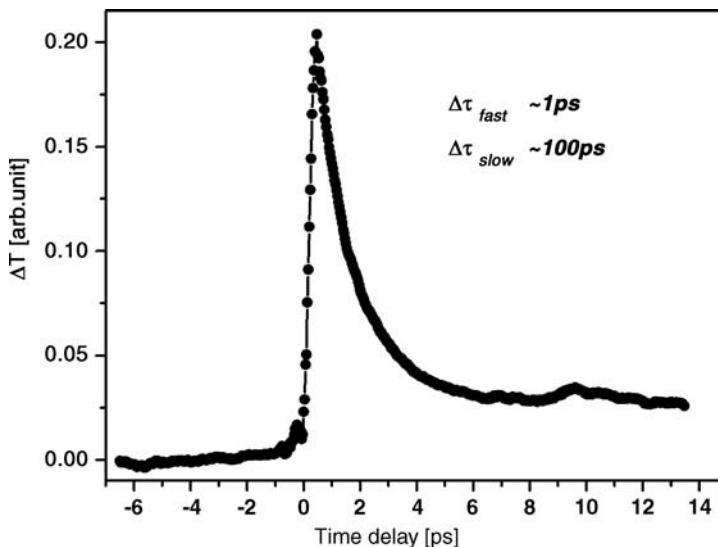


Figure 1.5 Pump-probe measurements of the carrier lifetime of a quantum dot waveguide device. $\Delta\tau_{fast}$ and $\Delta\tau_{slow}$ are fast and slow recovery times, respectively, and ΔT corresponds to the temporal changes in transmission.

repetition rates, where the absorption recovery should occur within the round-trip period of the cavity.

QDs suspended in glasses also exhibit fast carrier dynamics. Phonon bottleneck (see Section 2.3) has not been observed in these materials because of the existence of other relaxation channels for the carriers. These channels can be surface/defect states, electron–hole interaction in some materials [41], or multiphonon emission [42]. Their bleaching relaxation kinetics also exhibits a biexponential character, with fast and slow components, where the fast component decreases with reduction in the QD radius [35]. A review of all these dynamic processes can be found in Ref. [43].

2

Foundations of Quantum Dot Theory

A large number of theoretical papers on quantum dot structures, specifically lasers, have been published in the past decade or so. Here, we shall concentrate on those features and results that are the most relevant for the ultrafast behavior and short-pulse generation. Apologies are extended to colleagues whose work could not be included.

2.1

Energy Structure and Matrix Elements

As mentioned above, Stranski–Krastanov-grown quantum dots typically have a pyramidal shape (at least approximate), with quantization dimensions. Besides the dots, the active layer also contains one or several quantum wells (QWs), in the form of either the wetting layer or the technological QW in a dots-in-a-well (DWELL) system; below, we shall refer to the wells as wetting layer for definiteness.

It is impossible to solve Schrodinger equation for electrons and holes analytically in the three-dimensional pyramidal potential, so energy structure and interlevel transition matrix elements of quantum dots can be determined only numerically.

A typical result of such calculations, which agrees with experimental observations as discussed above, is that radiative transitions contributing to optical properties of epitaxial quantum dots typically involve electrons in at least two energy levels, referred to as the *ground level* (GL), located about 100 meV below the bandgap of the wetting layer, and the *excited level* (EL) or, more accurately, the *first* excited level, as shown in Figure 2.1. According to simulations, the ground state is a singlet state, with a degeneracy (entirely due to spin) of $Q_G = 2$. The excited state has a degeneracy, including spin, of $Q_E = 4$. A second excited level above the first excited level, with a degeneracy $Q_{E2} = 6$, is predicted by some theoretical calculations (see, for example, Ref. [44]); however, its effect on the optical properties of dots is less crucial. In most of the discussions below, we shall refer to just “the excited level,” meaning the first, or lowest, excited level. The reason for different degeneracy of levels as usual in quantum mechanics is the different symmetry of the wave functions of the ground and excited levels [45, 46], which also determine the highest overlap between the wave functions of the electrons and holes in the same state.

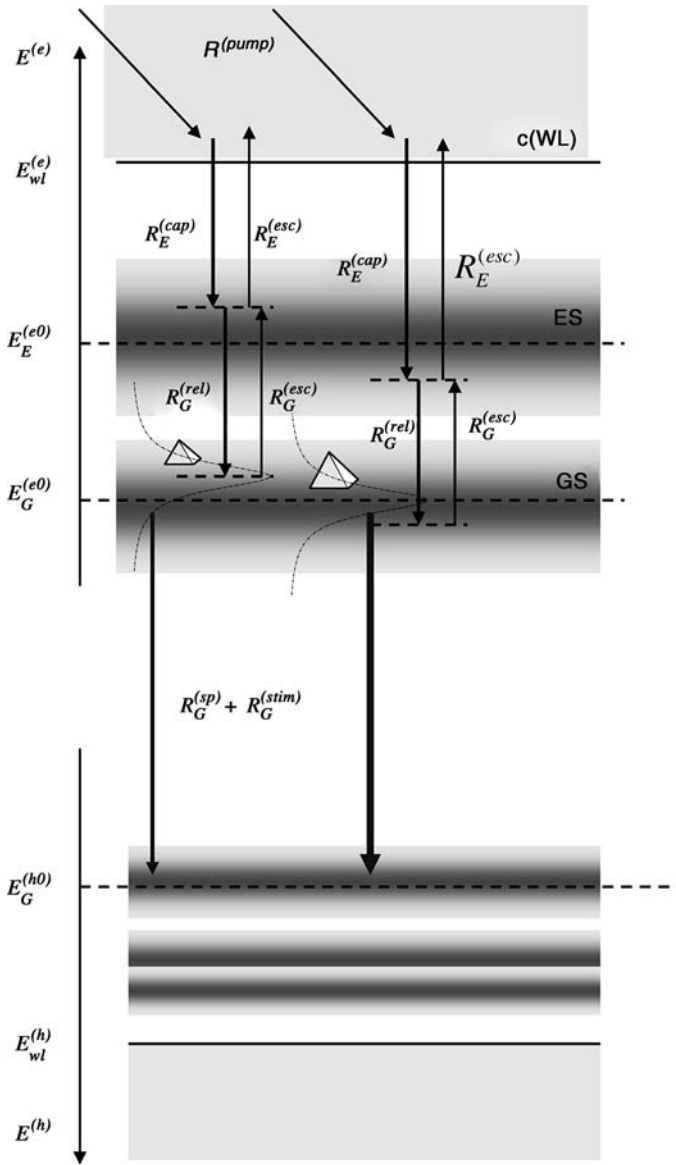


Figure 2.1 Schematic of level structure and the main electron kinetic processes in the most established dynamic model of a QD laser or amplifier. Stimulated transitions are assumed to affect the ground state only, and direct capture from the WL to the ground state is not included.

The energy structure for heavier holes may include a larger number of levels (up to 20 [47]), which is sometimes approximated as a continuum of energies.

Wave functions for electron and hole states allow the matrix elements of the optical transition to be calculated.

In the first approximation, for an infinitely deep potential, optical absorption or emission is possible only for the transition between a certain electron level and the hole level with the same quantum number. In practice, this rule is relaxed due to the finite potential depth and the mixing between heavy and light hole states, so that transitions between ground-level electrons and holes in excited levels are allowed [47]; however, ground- to ground-state transitions are still the most intense; the same may be expected for excited- to excited-state transitions.

A schematic of level structure involved in interpreting the QD dynamics is shown in Figure 2.1. Microscopic calculations of the energy levels and wave functions in the QDs, as well as the transition matrix elements constructed using these wave functions, have been reported in a large number of studies (see earlier monographs on quantum dots for an overview). The general tendency, as can be expected, is that, for dots of the same shape, the levels become deeper with the dot dimension. More precisely, the level position, counted from the dot material band edge, increases in a superlinear fashion as the dot becomes smaller (as in QWs, where the level position counted from the bandgap of the well material is roughly inversely proportional to the well thickness *squared*). An example of electron and hole ground energy levels, calculated for pyramidal InAs/GaAs dots as functions of the pyramid base (replotted after Ref. [33] using exponential fits proposed in that paper), is shown in Figure 2.2.

Microscopically calculated energy levels and transition matrix elements of quantum dots have also been directly used in some simulations on ultrafast dynamics [44]. With a better understanding of QD properties, such calculations may be hoped to gain full predictive capability. For the time being, their practical usefulness is limited by lack of knowledge of the dot shape, strain, and composition, particularly as, in order to take into account inhomogeneous broadening described in the previous

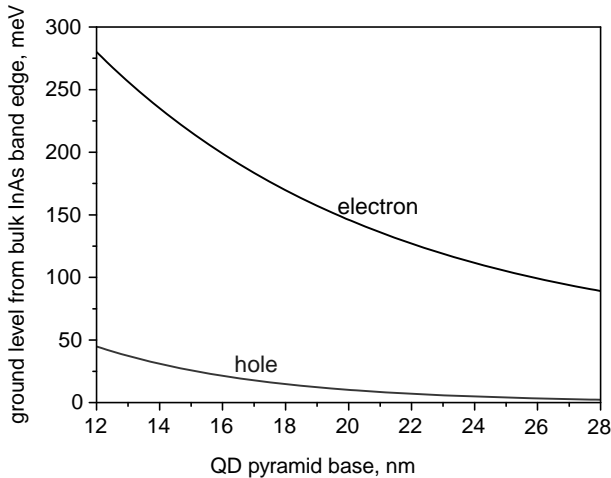


Figure 2.2 Calculated positions of the ground energy level for an electron and a hole in a pyramidal InAs/GaAs QD as functions of the pyramid base, measured from the InAs band edges. Adapted from Ref. [33].